Supplementary information

A versatile microfluidic tool for the 3D culture of HepaRG cells seeded at various stages of differentiation

Manon Boul[1,2,3,4,5], Nassima Benzoubir[2,4], Antonietta Messina[2,4], Rasta Ghasemi[5], Ismail Ben Mosbah[6], Jean-Charles Duclos-Vallée[2,4,7], Anne Dubart-Kupperschmitt[2,4], and Bruno Le Pioufle[*3,4,5]

[1]Université Paris Saclay, ENS Paris Saclay, CNRS SATIE, 4 avenue des Sciences, F91190 Gif-sur-Yvette, France
[2]UMR_S 1193 INSERM/Université Paris-Saclay, F94800 Villejuif, France
[3]Université Paris Saclay, ENS Paris Saclay, CNRS LUMIN, F91190 Gif-sur-Yvette, France
[4]FHU Hépatinov, Centre Hépato-Biliaire, Hôpital Paul Brousse, F94800 Villejuif, France
[5]Université Paris Saclay, Institut d'Alembert, ENS Paris Saclay, CNRS, F91190 Gif-sur-Yvette, France
[6]Biopredic International, Parc d'Affaires La Bretêche, 35760, Saint-Grégoire
[7]APHP, Centre Hépato-Biliaire, Hôpital Paul Brousse, F94800 Villejuif, France
*Correspondence and requests for materials should be addressed to B.L-P. (email: bruno.le-pioufle@ens-paris-saclay.fr)

Detailed SU8 mould fabrication

Supplementary Table S1.

Layer height [µm]	SU-8 type	Pre-baking time (65°C; 95°C; 65°C) [min]	UV exposure time [s]	Post-baking time (65°C; 95°C; 65°C) [min]	Developing time [min]
2	2002	1; 1; 1	6	1; 2; 1	1
5	2005	1; 2; 1	14	1; 2; 1	2
25	2025	1; 7; 1	16	1; 10; 1	5
40	2025	1; 7; 1	20	1; 10; 1	5

Detailed simulation method and additional results

Using COMSOL® software, we produced a 3D model of an array of 20 chambers in series with straight slits from the 40-2 µm device. The physical presence of cells was not taken into account. Water flowed within this structure at a temperature of 37°C and a creeping flow mode was chosen. A half flow rate of 400 nl/min was imposed at one inlet to the medium channel. The pressure was set at 0 Pa for the three outlets. Due to the computational time necessary for this 3D model to converge, the transport of oxygen could not be calculated under this simulation. A simpler model of one 3D chamber was then used. The values for fluid velocity and pressures at the input and outputs of the first, tenth, and twentieth chambers in the full simulation were taken and used in this new model. The transport of dilute oxygen species was coupled to the creeping flow mode. A block of material assumed to be PDMS surrounded the chamber and rose above it by 4 mm. The initial oxygen concentration was set at 0.2 mol/m^3 in both the fluid and PDMS and the diffusion coefficient was set at $1.8x10^{-9}$ cm^2/s in water and $3.25x10^{-9}$ cm^2/s in PDMS. The concentrations of oxygen at fluid input and at the surface of the PDMS the most distant from the circuit were kept at a constant value of 0.2 mol/m^3. Oxygen was consumed at a rate of $q_{O2} = 5x10^{-17}$ mol/s/cell through a Michaelis-Menten equation defined in the volume of the chamber, from its dead-end portion at -50 µm to its exit at 950 µm along its y axis (**Supplementary Fig. S1**): volumetric oxygen consumption rate in a chamber $OCR = q_{O2} \times Nc \times c_{O2} / (Vch \times (Km + c_{O2}))$, with c_{O2}, the oxygen concentration at a given point of the mesh[1-6]. The Michaelis constant Km value was set at 0.005 mol/m^3. The number of cells (Nc) within a chamber was set at 224 cells and the volume of the chamber (Vch) was $1.41x10^{-12}$ m^3.

Supplementary Figure S1. Fluid velocity and shear stress inside chambers of the 40-2 µm device for a flow rate of 400 nl/min. **a**) Diagram of one chamber. Velocity and shear stress values were measured in the middle of the chamber, along its y axis, from -50 µm to 950 µm (red line). **b**) Evolution of fluid velocity values in the middle of the chamber along its y axis (z = 20 µm) for chambers 1, 10, and 20. **c**) Evolution of shear stress values in the middle of the chamber along its y axis (z = 0 µm) for chambers 1, 10, and 20. **d**) Zoom on the evolution of the shear stress values shown in c) when the maximum shear stress was set at 0.1 Pa.

a

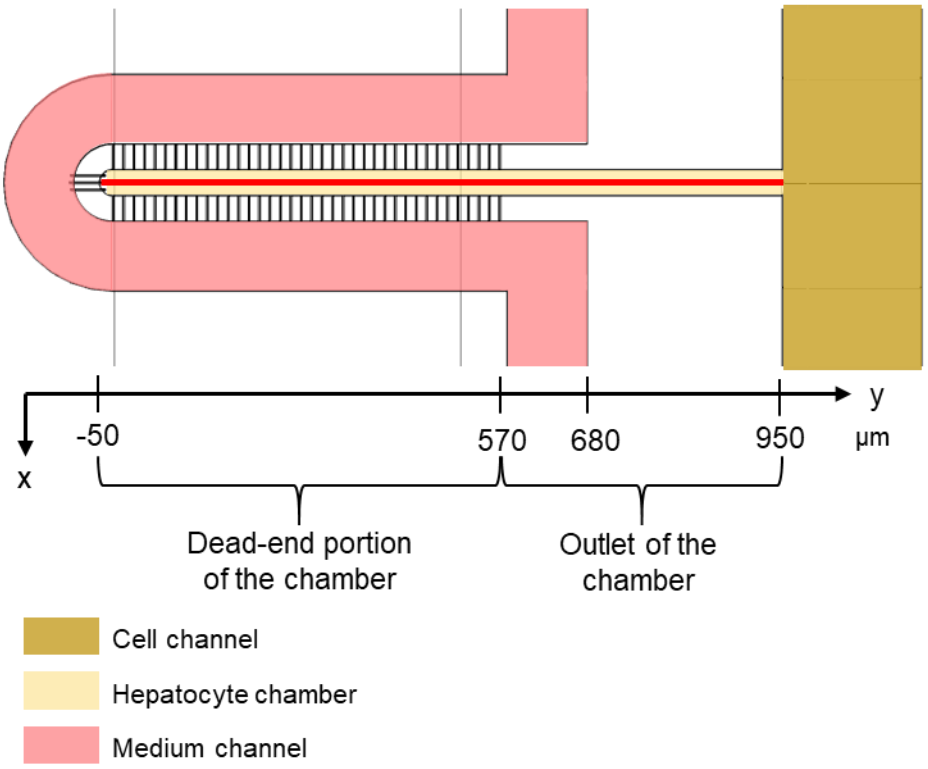
y
-50
570
680
950
µm
x
Dead-end portion of the chamber
Outlet of the chamber
Cell channel
Hepatocyte chamber
Medium channel

b

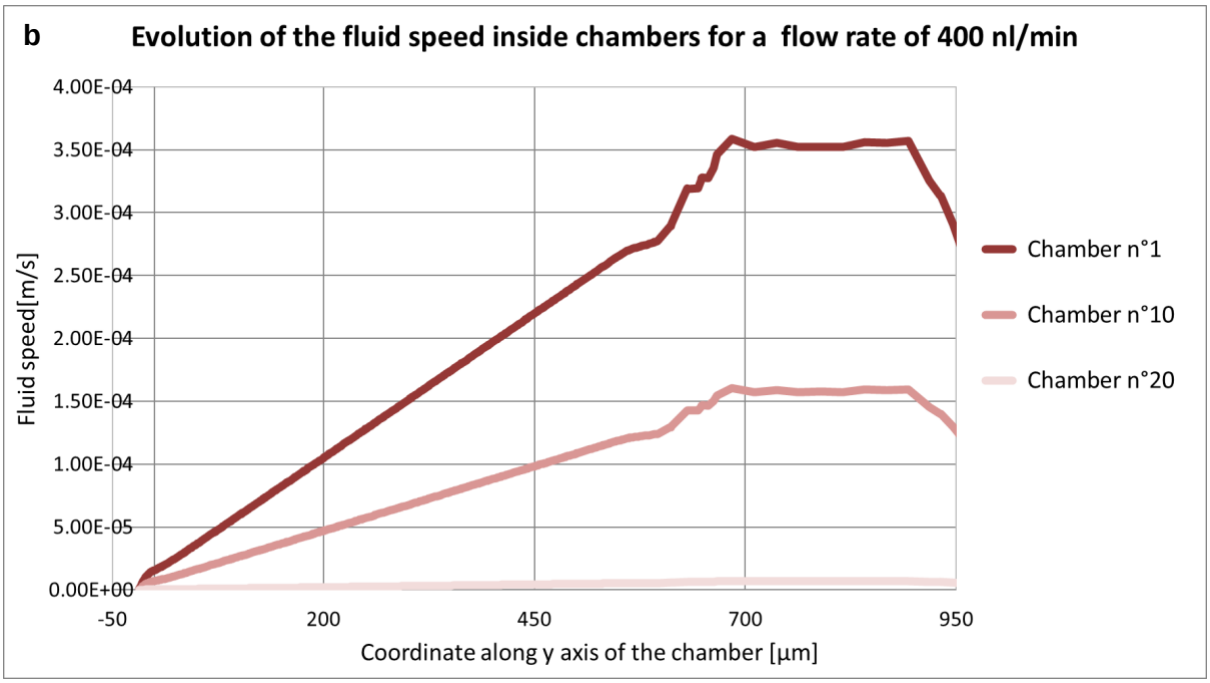
Evolution of the fluid speed inside chambers for a flow rate of 400 nl/min
4.00E-04
3.50E-04
3.00E-04
2.50E-04
2.00E-04
1.50E-04
1.00E-04
5.00E-05
0.00E+00
Fluid speed[m/s]
-50
200
450
700
950
Coordinate along y axis of the chamber [µm]
Chamber n°1
Chamber n°10
Chamber n°20

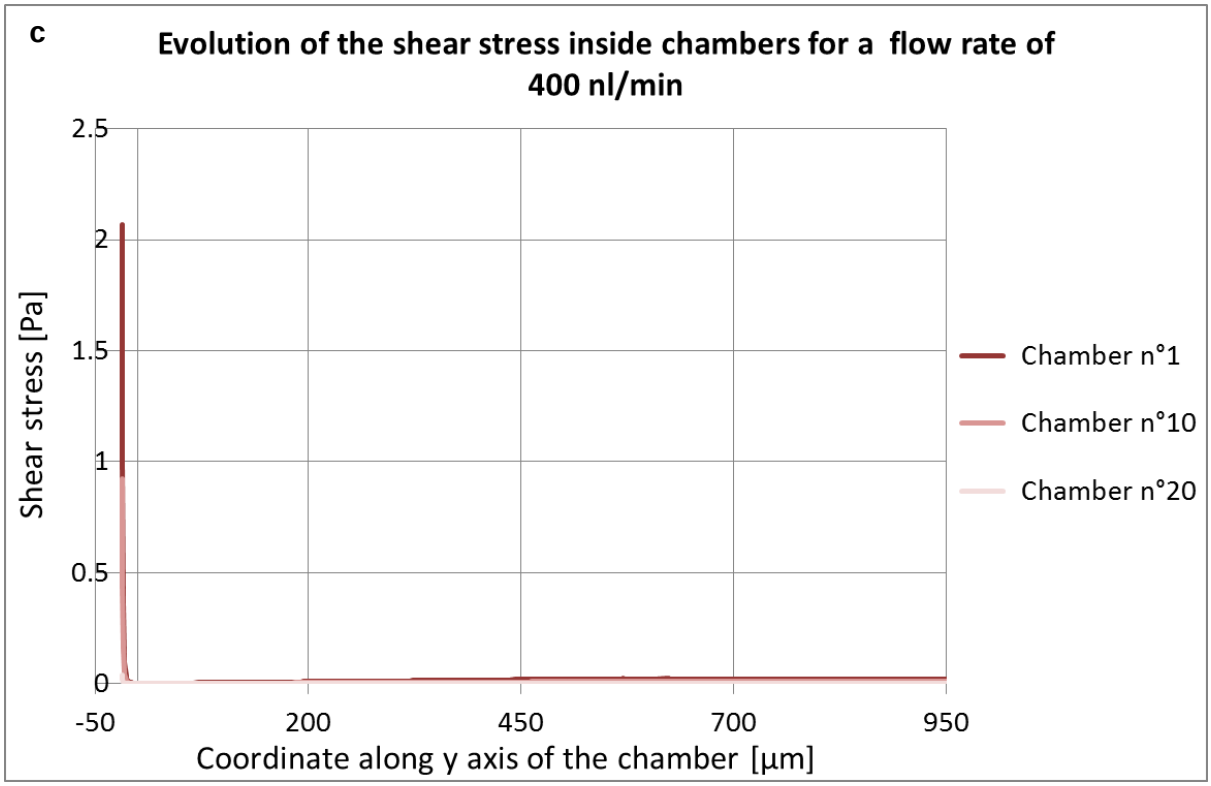
c
Evolution of the shear stress inside chambers for a flow rate of 400 nl/min
Shear stress [Pa]
2.5
2
1.5
1
0.5
0
-50
200
450
700
950
Coordinate along y axis of the chamber [µm]
Chamber n°1
Chamber n°10
Chamber n°20

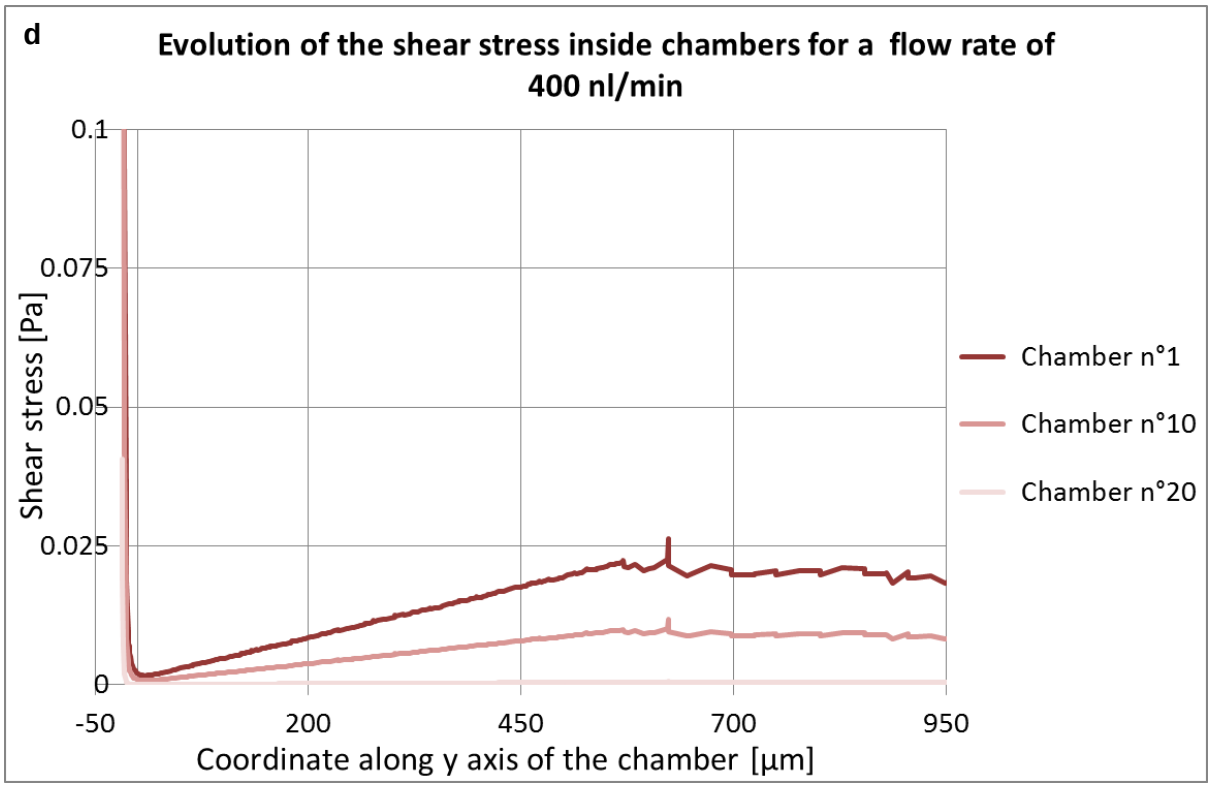
d
Evolution of the shear stress inside chambers for a flow rate of 400 nl/min
Shear stress [Pa]
0.1
0.075
0.05
0.025
0
-50
200
450
700
950
Coordinate along y axis of the chamber [µm]
Chamber n°1
Chamber n°10
Chamber n°20

Supplementary Figure S2. Evolution of oxygen concentrations in the middle of the chamber with the 40-2 µm design. The following cases are represented: first, oxygen is only diffusing from the medium channel input through the liquid (*No fluid convection, without diffusion through PDMS*). Then, a flow rate of 400 nl/min is set and oxygen is assessed in the different chambers (*Chambers 1, 10, and 20 without diffusion through PDMS*). Finally, the contribution of oxygen diffused through PDMS is added with either no flow or a 400 nl/min input flow (*No fluid convection + diffusion through PDMS* or *Chamber n°1 + diffusion through PDMS*, respectively).

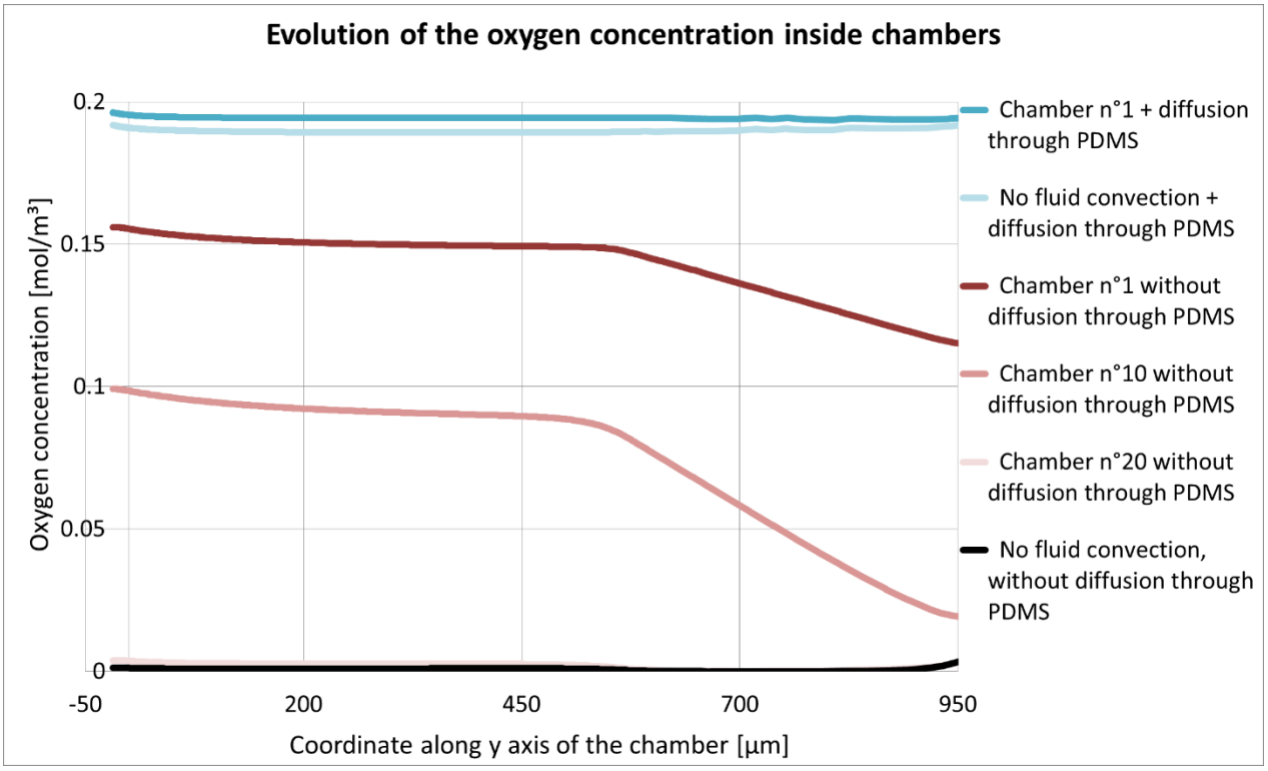

Evaluation of cell distribution with chambers after their culture period on the chip

Fiji software[7] was used to adjust the brightness and contrast of each fluorescence channel of the images acquired. The different optimised images were then merged. Within the image stacks in the chambers, fluorophore intensities decreased when moving from the glass slide to the upper PDMS surface. To obtain more uniform sectional images along the length of the chambers, the Stack Contrast Adjustment plugin[8] was used.

To determine the number of nuclei in the chambers, the DAPI maximum intensities of stacks were projected on the same plan and the nuclei counted manually. Epifluorescence microscope images with the same staining were also used. The portion of the chamber in which the cells were counted was between -50 to 680 µm along the y axis (**Supplementary Fig. S1**).

Supplementary Figure S3. Maximum intensity projection of cells stained with DAPI from 3D stacks (confocal microscopy). Examples of two different chambers. Scale bars = 40 µm.

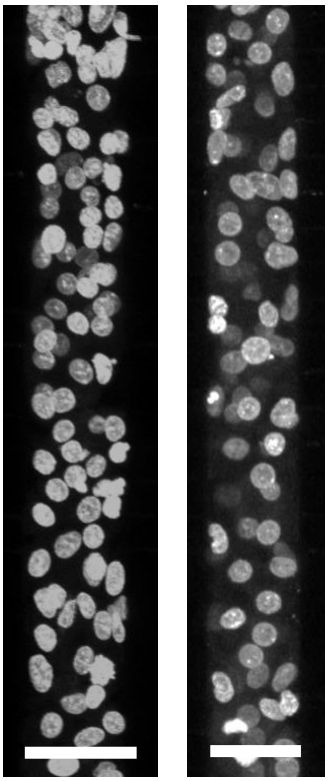

Detailed loading protocols

Supplementary Figure S4. Loading protocols. **a**) Suction was applied via the two outlets of the medium flow channels (blue arrows) and cells were deposited via the two inlets of the cell channel (green circles). **b**) Protocol change to maintain hepatocytes derived from HepaRG cells in the chambers: before suction was started, a medium-filled syringe connected to a hydraulic resistance (orange box) was connected to the medium channel. At the other extremity of this channel, an outlet tube (red line) was also connected and suction was then started by connecting it to the pressure controller (blue arrow). Cells were deposited as previously described (green circles). **c**) View of the system adapted for HepaRG hepatocytes. The syringe containing the cell culture medium is connected to the chip via tubes. The medium leaving the chip is collected to waste. To reduce the sensitivity of the device to pressure variations and be able to maintain the cells within the chambers, external high hydraulic resistances (red arrows) were added between the syringe and chip.

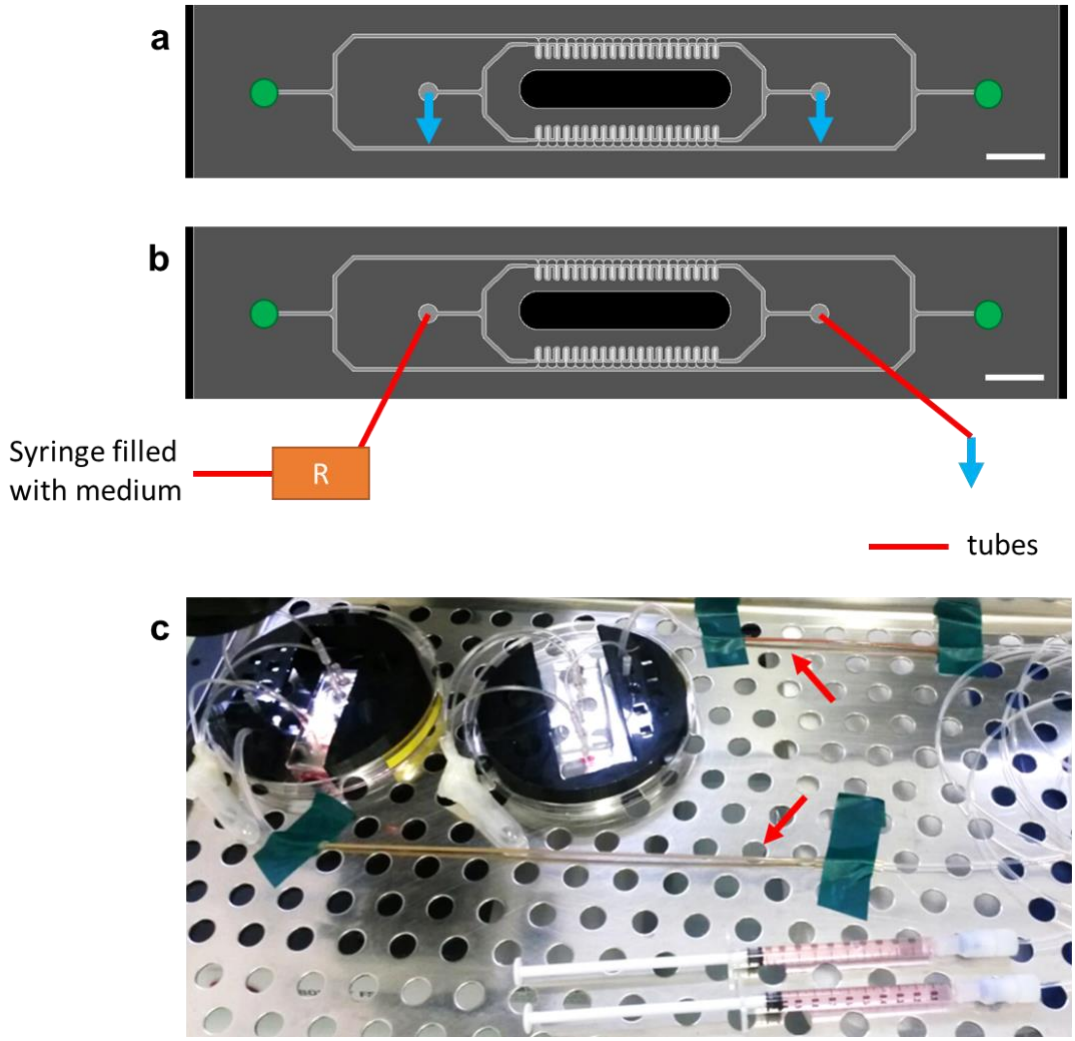

Detailed immunostaining protocol

The syringe (and resistance if present) was disconnected from the inlet of the chip medium channel. The three outlets were connected to a pressure controller. The different solutions were deposited at the inlet and suction was started. Suction and static periods were then alternated as detailed in **Supplementary Table 1**. To enable antibodies to reach all parts of the chip, two suction configurations were applied: n°1, as already described, and n°2, where the solutions were injected into one inlet of the cell channel and suctioned through the three outlets (**Supplementary Fig. S5**).

Supplementary Table S2. Sequence of solutions being deposited and suctioned at one inlet of the chip to perform immunostaining on the device.

Solutions to be suctioned	**Suction configuration**	**1st suction period [min]**	**1st static period [min]**	**2nd suction period [min]**	**2nd static period [min]**
PBS washing	1	10	5	5	5
Fixation with 4% PFA	1	10	10	5	10
PBS washing	1	10	5	5	5
Permeabilisation with triton solution	1	10	10	5	10
PBS washing	1	10	5	5	5
Blocking with 3% BSA	1	10	20	5	10
Primary antibodies	1	10	20	5	10
Primary antibodies	2	10	20	5	10
Overnight at 4°C					
PBS with tween washing	1	10	10	5	10
Secondary antibodies and DAPI	1	10	20	5	40
Secondary antibodies and DAPI	2	10	20	5	40
PBS with tween washing	1	10	10	5	10
H_2O washing	1	10	10	5	10
Chip imaging					

Supplementary Figure S5. Two suction configurations used during the immunostaining protocol. Liquids were deposited at one inlet (green circles) and suctioned using different values from three outlets (orange and blue arrows).

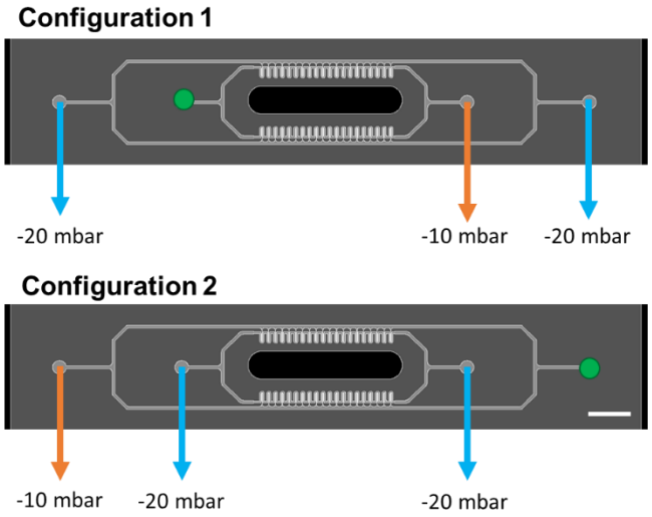

Supplementary Table S3. Table of antibodies used during experiments.

	Antibody	Host and isotype	Company	Catalogue n°	Dilution
Primary antibodies	ALB	Mouse	Sigma	A6684	1/200
	HNF4α	Rabbit	Santa Cruz	SC-8987	1/200
	ZO1	Rabbit	Novus Biologicals	NBP1-85047	1/200
Secondary antibodies	Alexa Fluor 488	Donkey anti-Mouse IgG	Fisher	A21202	1/1000
	Alexa Fluor 488	Donkey anti-Rabbit IgG	Fisher	A21206	1/1000
	Alexa Fluor 568	Donkey anti-Rabbit IgG	Fisher	A10042	1/1000
	Alexa Fluor 633	Donkey anti-Goat IgG	Fisher	A21082	1/1000
	Alexa Fluor 647	Donkey anti-Mouse IgG	Fisher	A31571	1/1000
	DAPI		Sigma	D9542	0.5 µg/ml
	Alexa Fluor 488 Phalloidin		Fisher	A12379	1/200
	Alexa Fluor 594 Phalloidin		Fisher	A12381	1/200

Supplementary Information References:

1. Bavli, D. *et al.* Real-time monitoring of metabolic function in liver-on-chip microdevices tracks the dynamics of mitochondrial dysfunction. *Proc. Natl. Acad. Sci.* (2016) doi:10.1073/pnas.1522556113.

2. Nahmias, Y. *et al.* A novel formulation of oxygen-carrying matrix enhances liver-specific function of cultured hepatocytes. *FASEB J.* (2006) doi:10.1096/fj.06-6192fje.

3. Matsumoto, S. *et al.* Integration of an oxygen sensor into a polydymethylsiloxane hepatic culture device for two-dimensional gradient characterization. *Sensors Actuators, B Chem.* (2018) doi:10.1016/j.snb.2018.05.053.

4. Grünig, D., Felser, A., Bouitbir, J. & Krähenbühl, S. The catechol-O-methyltransferase inhibitors tolcapone and entacapone uncouple and inhibit the mitochondrial respiratory chain in HepaRG cells. *Toxicol. Vitr.* (2017) doi:10.1016/j.tiv.2017.05.013.

5. Peyta, L. *et al.* Reduced cardiolipin content decreases respiratory chain capacities and increases ATP synthesis yield in the human HepaRG cells. *Biochim. Biophys. Acta - Bioenerg.* (2016) doi:10.1016/j.bbabio.2016.01.002.

6. Evenou, F., Fujii, T. & Sakai, Y. Spontaneous Formation of Highly Functional Three-Dimensional Multilayer from Human Hepatoma Hep G2 Cells Cultured on an Oxygen-Permeable Polydimethylsiloxane Membrane.

7. Schindelin, J. *et al.* Fiji: An open-source platform for biological-image analysis. *Nature Methods* (2012) doi:10.1038/nmeth.2019.

8. Čapek, M., Janáček, J. & Kubínová, L. Methods for compensation of the light attenuation with depth of images captured by a confocal microscope. *Microsc. Res. Tech.* (2006) doi:10.1002/jemt.20330.